



Article

Wear Behavior of Copper–Graphite Composites Processed by Field-Assisted Hot Pressing

Qian Liu ^{1,2} , Miguel Castillo-Rodríguez ², Antonio Julio Galisteo ³ ,
Roberto Guzmán de Villoria ^{2,4} and José Manuel Torralba ^{5,*}

¹ Hunan Provincial Key Laboratory of Health Maintenance for Mechanical Equipment, Hunan University of Science and Technology, Xiangtan 411201, China; qian.liu@imdea.org

² IMDEA Materials Institute, C/Eric Kandel 2, Getafe, 28906 Madrid, Spain; miguel.castillo@imdea.org (M.C.-R.); roberto.guzman@fidamc.es (R.G.d.V.)

³ Dpto. Matemática Aplicada, Ciencia e Ingeniería de Materiales y Tecnología Electrónica, Escuela Superior de Ciencias Experimentales y Tecnología, Universidad Rey Juan Carlos, C/Tulipan s/n, Móstoles, 28933 Madrid, Spain; antoniojulio.lopez@urjc.es

⁴ FIDAMC, Foundation for Research, Development and Application of Composite Materials, Avda. Rita Levi-Montalcini 29, Getafe, 28906 Madrid, Spain

⁵ Dpto. Ciencia e Ingeniería de Materiales e Ingeniería Química, Universidad Carlos III de Madrid, Av. de la Universidad 30, 28911 Leganés, Spain

* Correspondence: torralba@ing.uc3m.es; Tel.: +34-916-249-963

Received: 6 February 2019; Accepted: 18 March 2019; Published: 25 March 2019



Abstract: Copper–graphite composites with 0–4 wt % graphite were fabricated by field-assisted hot pressing with the aim of studying the effect of graphite content on microhardness and tribological properties. Experimental results reveal that hardness decreases with the graphite content. Wear testing was carried out using a ball-on-disc tribometer with a normal load of 8 N at a constant sliding velocity of 0.16 m/s. The friction coefficient of composites decreases significantly from 0.92 to 0.29 with the increase in graphite content, resulting in a friction coefficient for the 4 wt % graphite composite that is 68.5% lower than pure copper. The wear rate first increases when the graphite content is 1 wt %; it then decreases as the graphite content is further increased until a certain critical threshold concentration of graphite, which seems to be around 3 wt %. Plastic deformation in conjunction with some oxidative wear is the wear mechanism observed in pure copper, while abrasive wear is the main wear mechanism in copper–graphite composites.

Keywords: copper–graphite composites; field-assisted hot pressing; friction coefficient; wear

1. Introduction

Copper–graphite composites possess the positive properties of both components, i.e., the high thermal and electrical conductivity of copper with the low thermal expansion coefficient and good lubricating properties of graphite. Thus, copper–graphite composites constitute an attractive material for many applications, such as electrical brushes, bearings, and especially tribological engineering parts [1–3]. Several techniques have been used to produce copper–graphite composites, such as conventional powder metallurgy, microwave sintering, friction stir processing, and field-assisted sintering [4–9]. Generally, studies have shown that copper–graphite composites with finer particle sizes and better distribution exhibit higher load withstanding capacity and lower friction coefficient and wear rate due to a thick graphite layer that forms at the contact surface [5–7].

Copper–graphite composites are usually prepared by a powder metallurgy process that provides a uniform material at low production costs, but the process gives rise to a weak copper–graphite interface. This drawback can be overcome by coating the graphite particles with copper before consolidation.

Thus, Moustafa et al. [4] investigated the wear mechanism and friction coefficient of copper-graphite composites fabricated by powder metallurgy from Cu-coated and Cu-uncoated graphite particles containing 0–20 vol % graphite. They found that the copper-coated graphite composites exhibited the lowest friction coefficients and wear rates.

K. Rajkumar and S. Aravindan [6] produced copper-nanographite composites and copper-graphite composites by microwave sintering. They reported that nanographite-reinforced copper composites exhibited higher load withstanding capacity and a lower friction coefficient compared with copper-graphite composites. They argued that nanographite-reinforced composites have relatively smaller-sized asperities, as well as less space between the asperities that can be completely filled by nanographite particles during the wearing process. Then, a more continuous graphite layer which reduces the wear debris size is produced. D. Nayak and M. Debata [7] fabricated copper-graphite composites by the powder metallurgy route to study the effect of composition and milling time on the mechanical properties and wear resistance. They found that increasing the milling time yielded a better distribution and finer particle size, which led to a lower wear loss.

Samardi et al. [8] used friction stir processing to produce copper-graphite surface composites. They obtained a homogeneous particle distribution with no clusters. They found that compared with pure annealed copper, copper-graphite composites with 22 vol % graphite exhibited a friction coefficient that was 79% lower and a wear resistance that was about 65% higher.

Additionally, Samal et al. [9] prepared copper-graphite composites by the conventional powder metallurgy route using conventional and field-assisted sintering techniques. They reported that field-assisted sintering produced a better response to densification and hardening than conventional sintering. Thus, they obtained relative density values of 96% in the samples sintered by field-assisted hot pressing compared with 90% obtained in samples fabricated by conventional sintering. Moreover, the field-assisted sintered samples exhibited a Vickers hardness that was about 40% higher. Other researchers used field-assisted sintering techniques to fabricate uniformly distributed and dense copper-CNT (carbon nanotube) composites to study their thermal and electrical conductivity, hardness, and tensile properties [10,11]. Table 1 summarizes the mechanical properties of copper-graphite obtained by different authors and several techniques.

Table 1. Microhardness, average friction coefficient, and wear rate for copper-graphite composites. HV and BH stand for Vickers and Brinell hardness number, respectively. * Microhardness is given in BH for [4].

Ref.	System	Graphite Content	Microhardness (HV)	Friction Test Conditions (Load, Speed)	Friction Coefficient	Wear Rate (10 ⁻⁴ mm ³ /Nm)
[4]	Coated, cold pressing sintering	8 wt %	19.3 (BH) *	pin-on-ring	0.35	0.13
		15 wt %	16.4 (BH) *	100 N	0.25	0.14
		20 wt %	12.5 (BH) *	0.2 m/s	0.2	0.11
[5]	Hot isostatic pressing	30 vol %	-	pin-on-disc	0.15	16
		50 vol %	-	30 N, 0.5 m/s	0.15	5.7
[6]	Microwave sintering	15 vol %	72	pin-on-disc	0.22	0.5
		15 vol % (Nanographite)	81.5	12 N, 0.77 m/s	0.16	0.33
[7]	Ball milling, cold pressing, sintering	5 vol %	51	block-on-ring	-	4.97
		10 vol %	42	30 N, 1 m/s	-	1.11
		15 vol %	36		-	0.85
[8]	Friction stir processing	0 vol %	-	pin-on-disc	0.81	22.4
		6.54 vol %	-	10 N	0.45	15.4
		10.89 vol %	-	0.3 m/s	0.30	12.7
		16.70 vol %	-		0.22	11.3
		22.12 vol %	-		0.17	9.4
[9]	Conventional sintering	1 vol %	70	-	-	-
		3 vol %	70	-	-	-
		5 vol %	42	-	-	-
	Field-assisted sintering	10 vol %	50	-	-	-
		1 vol %	100	-	-	-
		5 vol %	100	-	-	-

In this study, copper and different amounts of graphite (0–4 wt %) were mixed by ball milling, and composites were fabricated by field-assisted hot pressing. The effect of graphite content on the microhardness and tribological properties of the obtained composites was investigated. Experimental results are discussed and compared with those previously reported in the literature.

2. Materials and Methods

2.1. Materials

Commercially available electrolytic copper powder with a dendritic shape and an average size of 15 μm was used as the matrix material. Graphite powder (JLQ ISMAF S.L., Spain), with 99.5% of the particles $<40 \mu\text{m}$ and 50% $<14 \mu\text{m}$, was used as reinforcement in the fabricated copper–graphite composites.

2.2. Composite Fabrication

The powder metallurgy route was used to fabricate the copper–graphite composites. Different weight fractions of graphite (0–4 wt %) were mixed with Cu powders by planetary ball milling (Pulverisette 6 classic, FRITSCH, Idar-Oberstein, Germany). The ball/powder ratio was 14:3, and powders were mixed at 300 rpm for 6 hours. The weight percentage used can be considered ca. 0–17% in volume percentage according to the density of Cu and graphite.

Field-assisted hot pressing (Gleeble 3800, DSI, Troy, NY, USA), also known as spark plasma sintering (SPS), was used to consolidate graphite–copper composites. The mixed powder was loaded into a cylindrical graphite die with an inner diameter of 20 mm. A sheet of graphitic paper was placed between the inside wall of the mold and the powders, as well as between the punch and the powders, to prevent any reaction between the powder and the mold material.

The sample was heated by passing current through the punches from room temperature to 980 °C at a heating rate of 100 °C/min. The holding time at 980 °C was 10 min. A pressure of 30 MPa was applied from 600 °C to the end of the sintering step. The cooling rate from the sintering temperature was 300 °C/min. Throughout the whole sintering process, the vacuum of the chamber was about 0.01 Pa. Henceforth in this work, specimens are referred to as Cu–nGr, where n is the weight percentage of graphite.

2.3. Microstructure Characterization

Fabricated composites were examined through Scanning Electron Microscope (EVO MA15, Zeiss, Oberkochen, Germany) with energy-dispersive X-ray spectroscopy (SEM with EDX). The density of the samples was determined by Archimedes' method according to the ASTM B962 standard. The theoretical densities of pure copper (8.9 g/cm³) and graphite (1.8 g/cm³) were used to calculate the relative density of the samples using the rules of mixtures.

2.4. Hardness Testing

The upper part of the specimens was polished with silicon carbide abrasive sandpaper until grit #2000. Indentation tests were performed on the polished surface of the specimens using a Vickers microhardness tester (SHIMAZU, HMV, Shimadzu Corp., Kyoto, Japan) with a 100 g load for 15 s in air at room temperature. At least five Vickers indentations were performed on each specimen type. The average microhardness values are shown in Table 1.

2.5. Tribological Performance Testing

The friction and wear experiments were performed using a ball-on-disc wear machine (CETR-UMT2, Bruker, Billerica, MA, USA) according to the ASTM G99-95 Standard. The steel ball used as the counterpart (AISI 316 stainless steel ball, Fe/Cr18/Ni10/Mo3) has a diameter of 6 mm and a higher hardness value than the tested material. A disc-shaped graphite–copper sample was tested

at room temperature in air with a relative humidity in the range of 40–50%. As the ASTM G99-95 standard does not designate the test parameters, such as load, rotation speed, or test duration, we performed preliminary testing to optimize the parameters. Finally, all the tests were carried out under the following conditions: contact load on the ball of 8 N, sliding speed of 0.16 m/s (320 rpm), 5 mm wear track radius, and 500 m as the total sliding distance. Each measurement was performed at least four times.

2.6. Wear Characterization

The value of the wear rate was calculated using the following formula [12]

$$W = \frac{\Delta V}{FS} \quad (1)$$

where W is the specific wear rate (mm^3/Nm), ΔV is the volume loss (mm^3), and F and S are the normal load (N) and the sliding distance (m), whose values in our tests were 8 N and 500 m, respectively.

The volume loss was measured from the weight loss and the sample density. However, since pure copper exhibited a very low wear rate compared with the other samples, a 3D Optical Profiler (Zeta-20 model from Zeta Instrument, Westborough, MA, USA) was used to calculate the volume wear from the worn track. Several cross-sectional profiles of the sample's worn track were assessed in order to evaluate the worn area and subsequently the loss volume produced during the wear test. A motorized sample platform was used, and several micrographs of each worn track were captured. A subsequent stitching method allowed us to obtain micrographs of large areas of the worn tracks.

3. Results and Discussion

3.1. Microstructure and Properties of Composites

Relative densities of about 98% or higher were measured in all sintered specimens (Table 2). These high values are in agreement with those typically achieved by field-assisted hot pressing [13,14].

Table 2. Properties of sintered composites

Material	Graphite Content (wt %)	Density (g/cm^3)	Relative Density (%)	Hardness (HV)	Friction Coefficient	Wear Rate ($10^{-4} \text{ mm}^3/\text{Nm}$)
Pure copper	0	8.76 0.06	98.4	94 ± 3	0.92 ± 0.09	0.03 ± 0.06
Cu-1Gr	1	8.41 ± 0.06	98.2	75 ± 2	0.33 ± 0.01	30.0 ± 2.7
Cu-2Gr	2	8.07 ± 0.02	97.8	72 ± 2	0.29 ± 0.02	14.6 ± 3.4
Cu-3Gr	3	7.90 ± 0.03	99.3	71.1 ± 1.4	0.3 ± 0.01	12.7 ± 3.8
Cu-4Gr	4	7.61 ± 0.06	98.9	69.7 ± 0.8	0.29 0.02	13.7 ± 3.0

Figure 1 shows typical micrographs of composites with 1–4 wt % graphite. There is no sign of porosity in the specimens. The dark gray contrast in the micrographs corresponds to graphite. Agglomerations of graphite are observed; the average size and surface density of the agglomerates were measured for each composite to study the graphite distribution in the copper matrix.

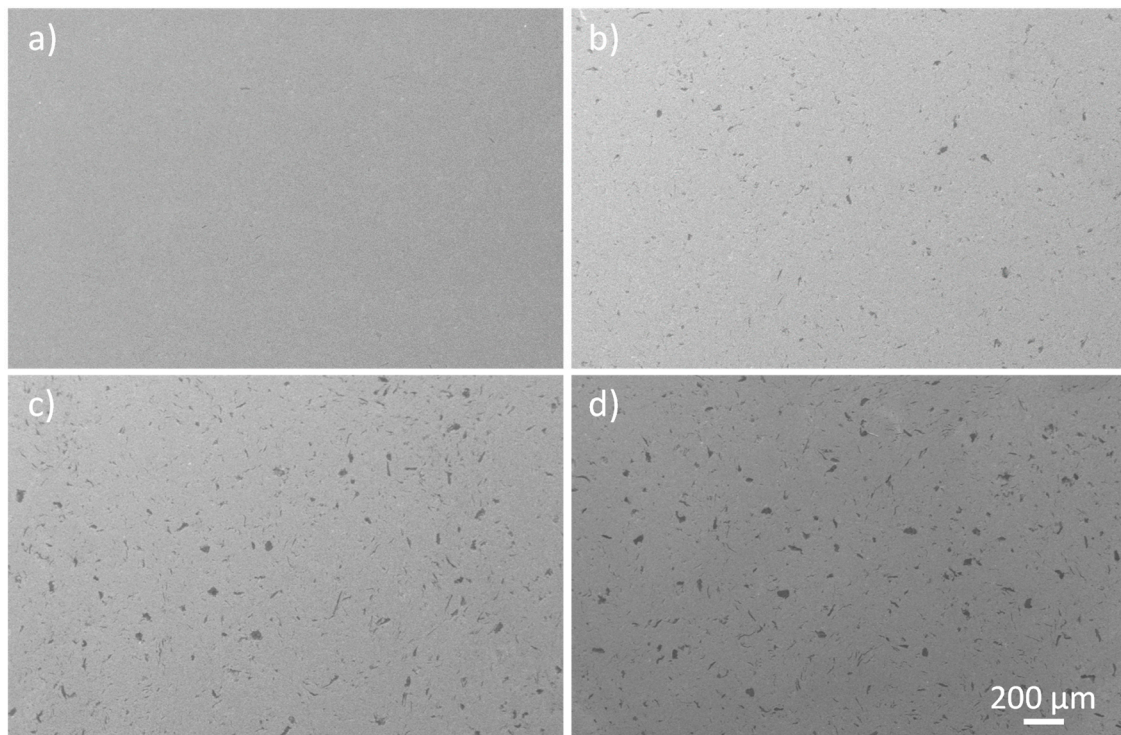


Figure 1. Scanning electron microscopy (SEM) images of (a) Cu-1Gr, (b) Cu-2Gr, (c) Cu-3Gr, and (d) Cu-4Gr.

The Cu-1Gr composite has very few graphite agglomerates. However, as more graphite is incorporated into the composites, agglomerates become clearly visible and have an average size of about 10 μm . The Cu-2Gr composites exhibit a surface density of graphite agglomerates of about 1.4% (0.28 wt %). Since the total amount of graphite for this composite is 2 wt %, we can conclude that about 14% of the total graphite is poorly dispersed around the Cu grains while forming agglomerates. The surface densities of the graphite agglomerates in the Cu-3Gr and Cu-4Gr composites are very similar and slightly increased to 2.1 and 2.3%, respectively. Therefore, for these composites, ~12–14% of the graphite forms agglomerates, but the rest is well dispersed in the copper matrix. Thus, the powder processing routine followed in this work leads to a moderately homogeneous dispersion of graphite in the copper matrix.

Since graphite is a soft material, a significant reduction in hardness is realized by adding 1 wt % graphite. The hardness of the composites slightly decreases with further increases in the amount of graphite, as was expected on the basis of previous studies [3–5,7,9] (Table 2): for example, Nayak and Debata [7] observed a decrease in hardness from 51 HV to 36 HV when the graphite content increased from 5 vol % to 15 vol %. The composites in the present study exhibit higher hardness values (ca. 70 HV) compared with the composites fabricated by cold pressing followed by 1 hour of sintering, but their values are similar to those of composites fabricated using microwave sintering, considering similar levels of reinforcement.

Samal et al. [9] studied the hardness of Cu-graphite (1 and 10 vol %, i.e., about 0.2 and 2 wt %) fabricated by field-assisted hot pressing and conventional techniques. Our hardness measurement results for pure copper are very close to what they obtained. However, our results for the Cu-Gr composites are slightly higher than those obtained by conventional sintering. The reason for these differences in samples with the same composition likely lies in the samples' grain size, which strongly depends on the sintering technique. Thus, the high heating rate with the short sintering time results in a fine grain size, which is responsible for the improvement in the hardness value [9].

3.2. Friction and Wear Behavior

Figure 2 shows the SEM images of the wear tracks of the pure copper sample. In our tests, the applied normal load was 8 N using a stainless-steel ball as the counterbody. Because of the geometrical shape of the ball, the initial contact area was very limited, but as the test proceeded and the wear occurred, this contact area increased, and consequently, the stress applied to the material decreased. Therefore, a considerable plastic deformation with some adhesive wear is observed in the center of the wear track (Figure 2a). The main wear mechanism observed in the material is plastic deformation, as clearly seen in both the SEM and 3D optical profiler micrographs of the worn track (Figure 2a,c), with the lateral zone of the track clearly showing a pile-up effect. Also, the EDX analysis shows a clear oxygen peak in the worn track in the EDX zone marked B (Figure 2b), confirming the existence of an oxidative wear mechanism as well, as was also found by Moustafa et al. [4]. They studied the wear mechanism of pure copper and copper–graphite using a wide load range (50–500 N). With the low wear regime, as in the present work, they found that oxidation-delamination was the operating wear mechanism in pure copper. They also observed fine particles consisting of copper and Cu_2O from the debris of pure copper samples.

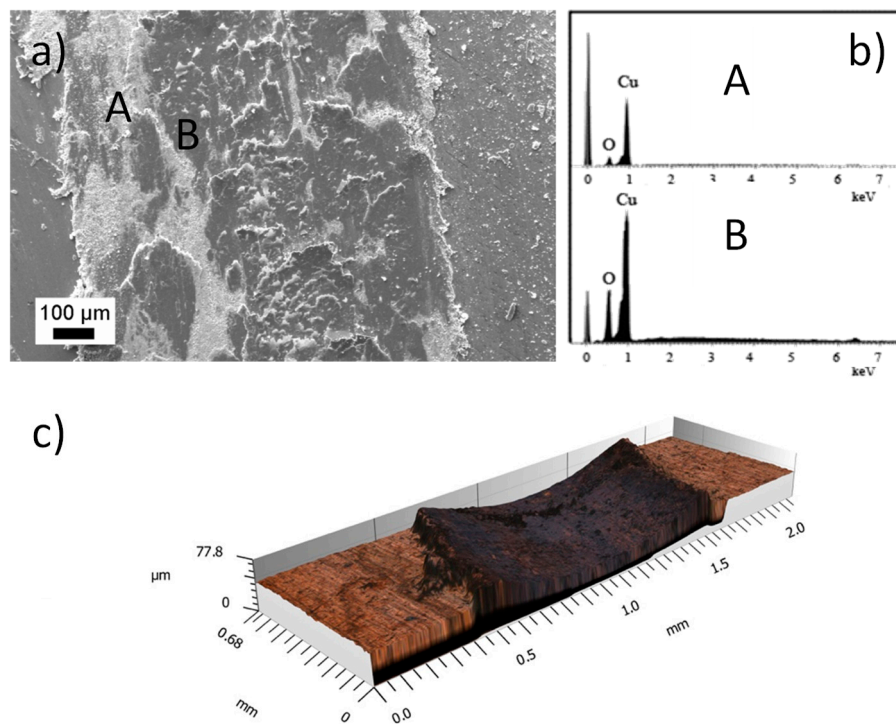


Figure 2. (a) SEM images of the wear track of the pure copper sample, where Energy Dispersive X-ray Spectroscopy (EDS) spectra performed in regions A and B are shown (b). 3D optical profiler micrograph of the worn track, where axis units are in microns (c).

In the present work, the load used was even lower than that in the above study, promoting the formation of a mechanically mixed layer (MML) as a result of deformed oxidized copper protecting the material to be worn. Usually, when these oxides are produced between the ball and the substrate, a ‘three bodies’ wear mechanism is initiated because of the fragile behavior of the oxide, with significant increases in the wear rate and clear plowing grooves in all directions in the worn track. The plastic deformation of the Cu debris produces an adhesive phenomenon on the wear track that prevents the progression of the ‘three bodies’ wear mechanism, which is usually more aggressive than any other wear mechanism, as observed in Figure 2a.

In copper–graphite composites, the situation is different as a result of the presence of graphite. The role of graphite in tribological behavior can be summarized as follows: due to their softness and

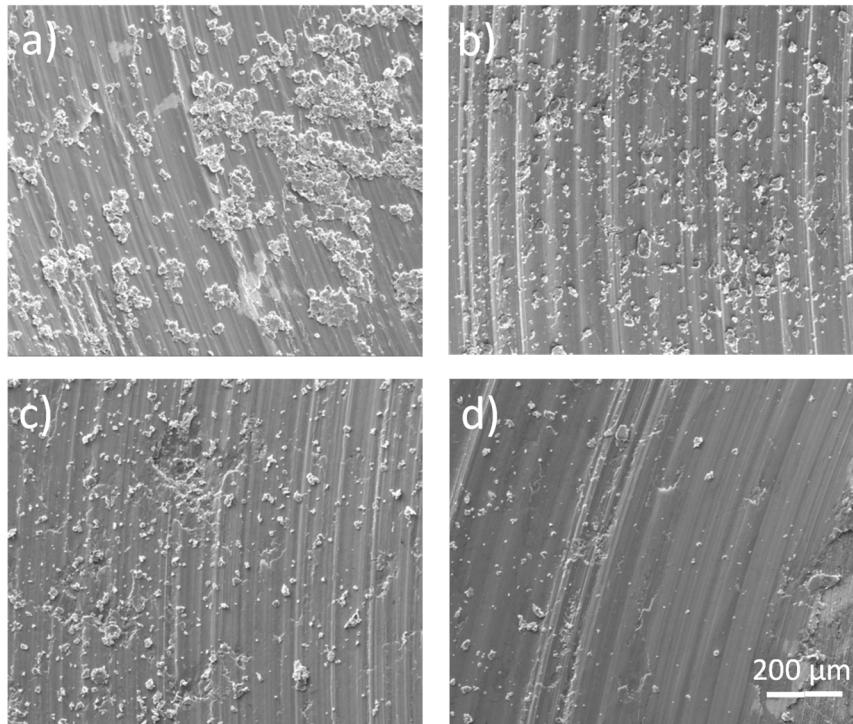
lamellar structure, graphite particles in the subsurface deform with the subsurface matrix and are squeezed out to the wearing surface during the sliding friction process. Then, the graphite smears the wearing surface layer by layer and mixes with the other debris detached from the contacting face. This mechanical mixing process results in the formation of an MML rich in graphite [15]. Graphite is a natural lubricating material used in solid bearings. In the composite system reported in this work, graphite acts in the same way by introducing a soft lubricant phase between the counterpart and the worn surface. Graphite also reduces the wear effect; however, some hard particles, such as copper oxide particles, are present in the tribological system.

As previous studies have pointed out, the size, volume fraction, and homogeneity of the distribution of graphite have significant effects on the formation of the graphite-rich layer [4,5]. Firstly, a finer size of graphite particles leads to a lower wear rate and friction coefficient for the same graphite concentration. For example, copper-graphite composites with 16 μm graphite particles [5] had a lower friction coefficient than composites with 40 μm graphite particles [4]. Moreover, Rajumar et al. [6] reported that copper composites with 35 nm nanographite had a higher wear resistance and lower friction coefficient compared with composites containing 50 μm graphite particles. In our work, the graphite powder comprises particles with sizes lower than 40 μm , and consistent with the above, our friction coefficient values are lower than those in [4] but higher than the values reported in [5]. Secondly, the amount of graphite added to the matrix could directly affect the thickness and extent of the graphite-rich layer, which plays an important role in the wear behavior of composites. As the amount of graphite addition increases, more graphite is released to the wear surface smeared on the layer. Therefore, the graphite-rich layer on the contact surface becomes thicker and denser [16]. With increased graphite content, this layer can effectively decrease the friction coefficient and the wear. Many similar results have been observed not only in the copper matrix but also in other metal matrices [17–20]. However, it is confirmed that with an increasing graphite fraction, the friction coefficient and wear rate decrease until a critical threshold of graphite concentration is reached [5]. This threshold concentration is 23 vol % (5.7 wt %) for graphite sizes between 40 and 25 μm , 12 vol % (2.7 wt %) for a graphite size of about 16 μm [5], and approximately 15 vol % (3.4 wt %) for graphite with a nanosize of 35 nm [6]. Beyond this threshold concentration, the friction coefficient becomes almost independent of the composition; in fact, copper-nanographite composites can even show a higher friction coefficient and wear rate due to the agglomeration of nanographite particles.

Figure 3 shows the wear tracks of composites with graphite content ranging from 1 to 4 wt %. In the case of Cu-1Gr (Figure 3a), an adhesive wear mechanism in conjunction with an abrasive phenomenon on the surface is observed. Particles detached from the copper adhered to the counterpart are then transferred to the wear track, and because of the limited lubricating effect in this sample due to the small quantity of graphite, several zones of attached particles are observed in the wear track, together with some abrasion grooves (Figure 3a). The main wear mechanism of this Cu-1Gr specimen is adhesion. In Cu-2Gr (Figure 3b), many wide grooves along the sliding direction can be observed, revealing that abrasion is the main wear mechanism in this sample. The number and size of adhered particles are decreased in comparison with the Cu-1Gr sample. The increase in graphite content lubricates the wear track, and some debris particles are not transferred to the final track. When the graphite content increases to 3 wt % in the Cu-3Gr composite, the abrasion grooves become slimmer, as shown in the worn surface (Figure 3c), which indicates that there is a sufficient amount of graphite to increase the self-lubricating effect at the contact surface. The adhesive wear mechanism can hardly be observed. The Cu-4Gr composite shows a smooth worn surface with small wear scars: these characteristics indicate that a thick graphite-rich layer is formed (Figure 3d). EDX analysis was used to determine the carbon content on the worn surface. Table 3 shows the results of EDX analysis of the copper-graphite composites. The increased weight and atomic percent of carbon detected on the surface indicate that the graphite-rich layer is enhanced by increasing the graphite content.

Table 3. Results of Energy Dispersive X-ray Spectroscopy (EDS) analysis of the worn surface of copper–graphite composites.

Material	Weight%		Atomic%	
	C	Cu	C	Cu
Cu-1Gr	2.11	97.89	9.55	90.45
Cu-2Gr	5.64	94.36	24.02	75.98
Cu-3Gr	8.06	91.94	31.68	68.32
Cu-4Gr	12.56	87.44	46.53	53.47

**Figure 3.** SEM images of the wear track of copper–graphite composites, (a) Cu-1Gr, (b) Cu-2Gr, (c) Cu-3Gr, and (d) Cu-4Gr.

The variation in the friction coefficient as a result of increasing the graphite content is shown in Table 2. A sharp decrease in the friction coefficient is observed: from 0.92 in pure copper to 0.32 in Cu-1Gr. Further increasing the graphite content does not significantly change the friction coefficient, whose value is in the range of 0.29–0.3. This reduction in the friction coefficient of copper–graphite composites could be attributed to the presence of the graphite layer on the sliding surface of the wear sample since the graphite layer decreases the metal–metal contact points.

Figure 4 shows the changes in the friction coefficient as a function of the sliding distance for different tested specimens. The substantial noise on the curve of pure copper reflects that the contact lacks stability. Meanwhile, the Cu-3Gr and Cu-4Gr curves present little noise, which indicates a much more stable contact.

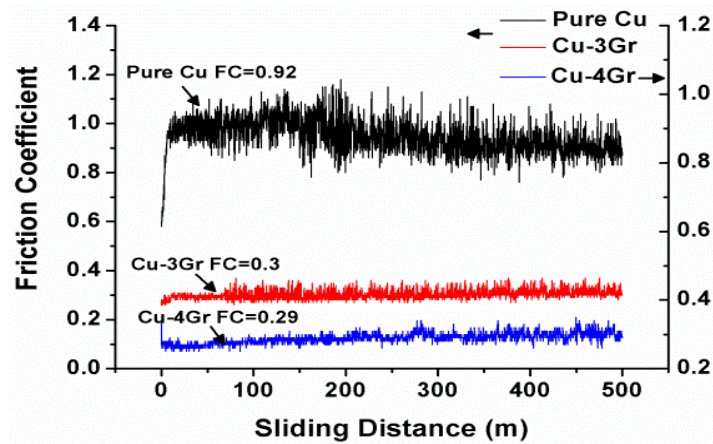


Figure 4. Friction coefficient variations as a function of graphite content.

Pure copper exhibits a very low wear rate value compared with the samples containing graphite (Table 2), where the wear rate is calculated from the weight loss of the samples before and after the wear test. Then, several cross-sectional profiles of the sample worn track were examined to investigate the reason for such wear behavior. Figure 5 shows the cross-sectional profile for pure copper; the profiles related to the composites are included for the sake of comparison. From this figure, it is observed that when the pure copper sample slides against the counterpart in a low wear regime, because of its ductility, the copper debris formed is plastically deformed on the contacting surface, then repeatedly pressed on the wear track by the counterpart, and finally transferred to the wear track. This, together with the oxidation of the copper, is the reason that the weight loss and thus the wear rate value is so small in this sample. In any case, wear damage appears on pure copper, and the wear resistance of this material is low in the tested conditions, although very little penetration of the copper by the counterbody is observed in the cross-sectional profile (Figure 5), and because the weight loss is also small, this leads to a very low specific wear rate (Table 2).

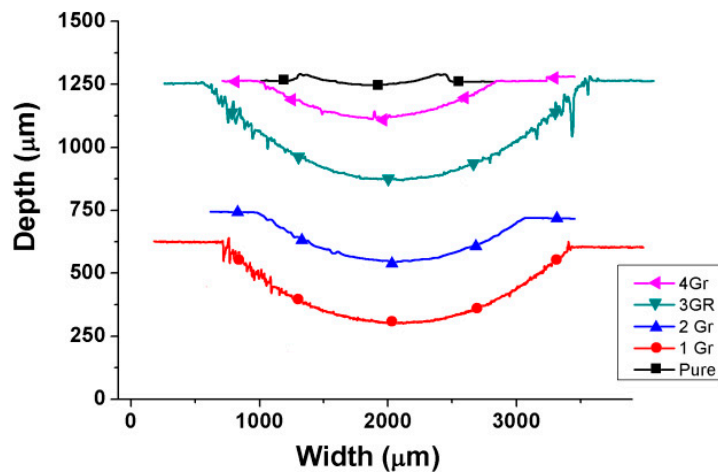


Figure 5. Cross-sections of the worn tracks for pure copper and the composite specimens. For comparative purposes, the curves of the different specimens are offset on the *y*-axis.

However, the presence of graphite improves the mobility of the debris as a result of the self-lubrication effect of graphite, and it is difficult for the debris to adhere to the wear surface of the composite compared with that of the pure copper sample. It is interesting that copper with 1 wt % graphite has the highest weight loss (see Table 2). The reason for this may be that by adding 1 wt % graphite, the hardness of the composite decreases and the mobility of the debris improves, but the amount of graphite is insufficient to form a uniform graphite-rich layer. With the increase in

graphite content, as mentioned previously, the wear surface is gradually covered with a graphite-rich layer, and the wear loss of the composites decreases, as seen in the cross-sectional profiles in Figure 5. Further increasing the graphite content (2–4 wt %) has a slight effect on the wear loss of the composites. Similar results have also been reported by other researchers using the conventional sintering route [4,7].

In Cu–3Gr, the lowest wear rate of $12.7 \times 10^{-4} \text{ mm}^3/\text{Nm}$ is obtained, which seems to indicate a threshold graphite concentration of about 3 wt % under our experimental conditions. The value of this threshold is in agreement with Kovacic et al.'s study [5]. However, the existence of this threshold concentration of 3 wt % graphite could be more clearly demonstrated in our work by investigating the tribological behavior of composites containing higher graphite amounts.

4. Conclusions

Pure copper and copper samples containing 1–4 wt % graphite were fabricated by field-assisted hot pressing. Dense and porosity-free samples were obtained with a moderately homogeneous distribution of graphite in the copper matrix. The presence of graphite has a strong influence on the microhardness and tribological properties. The hardness of the samples decreases with the addition of graphite. On the basis of the ball-on-disc tribological test, it is concluded that graphite drastically reduces the friction coefficient: the composite containing 4 wt % graphite exhibits a friction coefficient that is 68% lower than that of pure copper. The wear rate first increases when the graphite content is 1 wt %, and then it decreases with further increases in the graphite content until a certain critical graphite threshold concentration, whose value seems to be around 3 wt %. Plastic deformation with subsequent adhesion and transference is the main wear mechanism in pure copper, whereas, in copper–graphite composites, the dominant mechanism is abrasive wear.

Author Contributions: Conceptualization, J.M.T., R.G.d.V.; Methodology, R.G.d.V., and J.M.T.; Investigation, Q.L., A.J.G., and M.C.-R.; Writing—Original Draft Preparation, Q.L.; Writing—Review & Editing, Q.L., M.C.-R., A.J.G., R.G.d.V., and J.M.T.; Supervision, J.M.T.

Funding: This research was financially supported by the National Natural Science Foundation of China (No. 51704113). R.G.d.V. would like to thank the Community of Madrid for financial support through the NMT2D-CM (S2018/NMT-4511) and the TEMACON project.

Conflicts of Interest: The authors declare no conflict of interest.

References

- Zahran, R.R.; Ibrahim, I.H.M.; Sedahmed, G.H. The corrosion of graphite/copper composites in different aqueous environments. *Mater. Lett.* **1996**, *28*, 237–244. [[CrossRef](#)]
- Kestursatya, M.; Kim, J.K.; Rohatgi, P.K. Wear performance of copper–graphite composite and a leaded copper alloy. *Mater. Sci. Eng. A* **2003**, *339*, 150–158. [[CrossRef](#)]
- Ma, X.; He, G.; He, D.; Chen, C.; Hu, Z. Sliding wear behavior of copper–graphite composite material for use in maglev transportation system. *Wear* **2008**, *265*, 1087–1092. [[CrossRef](#)]
- Moustafa, S.; El-Badry, S.; Sanad, A.; Kieback, B. Friction and wear of copper–graphite composites made with Cu-coated and uncoated graphite powders. *Wear* **2002**, *253*, 699–710. [[CrossRef](#)]
- Kováčik, J.; Emmer, Š.; Bielek, J.; Keleši, L. Effect of composition on friction coefficient of Cu–graphite composites. *Wear* **2008**, *265*, 417–421. [[CrossRef](#)]
- Rajkumar, K.; Aravindan, S. Tribological behavior of microwave processed copper–nanographite composites. *Tribol. Int.* **2013**, *57*, 282–296. [[CrossRef](#)]
- Nayak, D.; Debata, M. Effect of composition and milling time on mechanical and wear performance of copper–graphite composites processed by powder metallurgy route. *Powder Metall.* **2014**, *57*, 265–273. [[CrossRef](#)]
- Sarmadi, H.; Kokabi, A.; Reihani, S.S. Friction and wear performance of copper–graphite surface composites fabricated by friction stir processing (FSP). *Wear* **2013**, *304*, 1–12. [[CrossRef](#)]
- Samal, C.; Parihar, J.; Chaira, D. The effect of milling and sintering techniques on mechanical properties of Cu–graphite metal matrix composite prepared by powder metallurgy route. *J. Alloys Compd.* **2013**, *569*, 95–101. [[CrossRef](#)]

10. Chu, K.; Wu, Q.Y.; Jia, C.C.; Liang, X.B.; Nie, J.H.; Tian, W.H.; Gai, G.S.; Guo, H. Fabrication and effective thermal conductivity of multi-walled carbon nanotubes reinforced Cu matrix composites for heat sink applications. *Compos. Sci. Technol.* **2010**, *70*, 298–304. [[CrossRef](#)]
11. Daoush, W.M.; Lim, B.K.; Mo, C.B.; Nam, D.H.; Hong, S.H. Electrical and mechanical properties of carbon nanotube reinforced copper nanocomposites fabricated by electroless deposition process. *Mater. Sci. Eng. A* **2009**, *513–514*, 247–253. [[CrossRef](#)]
12. Czichos, H.; Klaffke, D.; Santner, E.; Woydt, M. Advances in tribology: The materials point of view. *Wear* **1995**, *190*, 155–161. [[CrossRef](#)]
13. Sule, R.; Olubambi, P.; Sigalas, I.; Asante, J.; Garrett, J. Effect of SPS consolidation parameters on submicron Cu and Cu–CNT composites for thermal management. *Powder Technol.* **2014**, *258*, 198–205. [[CrossRef](#)]
14. Liu, Q.; He, X.B.; Ren, S.B.; Zhang, C.; Liu, T.T.; Qu, X.H. Thermophysical properties and microstructure of graphite flake/copper composites processed by electroless copper coating. *J. Alloys Compd.* **2014**, *587*, 255–259. [[CrossRef](#)]
15. Zhan, Y.; Zhang, G. Friction and wear behavior of copper matrix composites reinforced with SiC and graphite particles. *Tribol. Lett.* **2004**, *17*, 91–98. [[CrossRef](#)]
16. Akhlaghi, F.; Zare-Bidaki, A. Influence of graphite content on the dry sliding and oil impregnated sliding wear behavior of Al 2024–graphite composites produced by in situ powder metallurgy method. *Wear* **2009**, *266*, 37–45. [[CrossRef](#)]
17. Hocheng, H.; Yen, S.; Ishihara, T.; Yen, B. Fundamental turning characteristics of a tribology-favored graphite/aluminum alloy composite material. *Compos. Part A* **1997**, *28*, 883–890. [[CrossRef](#)]
18. Riahi, A.; Alpas, A. The role of tribo-layers on the sliding wear behavior of graphitic aluminum matrix composites. *Wear* **2001**, *251*, 1396–1407. [[CrossRef](#)]
19. Teoh, S.; Thampuran, R.; Seah, W. Coefficient of friction under dry and lubricated conditions of a fracture and wear resistant P/M titanium-graphite composite for biomedical applications. *Wear* **1998**, *214*, 237–244. [[CrossRef](#)]
20. Li, J.L.; Xiong, D.S. Tribological properties of nickel-based self-lubricating composite at elevated temperature and counterface material selection. *Wear* **2008**, *265*, 533–539. [[CrossRef](#)]



© 2019 by the authors. Licensee MDPI, Basel, Switzerland. This article is an open access article distributed under the terms and conditions of the Creative Commons Attribution (CC BY) license (<http://creativecommons.org/licenses/by/4.0/>).